The Morphology of Irradiated Isotactic Polypropylene

X. C. ZHANG, R. E. CAMERON

University of Cambridge, Department of Materials Science and Metallurgy, New Museums Site, Pembroke Street, Cambridge, CB2 3QZ, United Kingdom

Received 13 November 1998; accepted 11 May 1999

ABSTRACT: The research in this article explores the response of semicrystalline isotactic polypropylene to gamma radiation in air, and relates the morphological changes of the polymer to corresponding changes in mechanical properties. The effect of the initial morphology of the polymer on its response to irradiation is considered using infrared spectroscopy (FTIR), small- and wide-angle X-ray scattering, dynamic mechanical thermal analysis (DMTA), and mechanical testing. The extent of chain scission and crosslinking is dependent on the dose but not the initial starting morphology. These chemical changes cause the crystallinity to increase slightly, and the glass transition temperature to rise by a few degrees in all samples, but the overall morphology is only subtly changed. In contrast, a major deterioration in mechanical properties is caused. The effects of the irradiation observed under these conditions are similar in each material and the ultimate properties determined by the properties seen in the original material. © 1999 John Wiley & Sons, Inc. J Appl Polym Sci 74: 2234–2242, 1999

Key words: gamma irradiation; isotactic polypropylene; semicrystalline morphology

INTRODUCTION

Isotactic polypropylene may crystallize into one three isomorphs, termed α, β, and γ.[1] Conventional thermal processing results in the α isomorph, which is monoclinic in symmetry.[1] The crystals are lamellar in form, and the arrangement of these lamellae is a function of the crystallization temperature. According to Keith and Padden,[2] if crystallized above 138°C, the spherulites have a negative birefringence, indicating that the lamellae are arranged radially within them. However, spherulites crystallized below 134°C have positive birefringence that can only be explained if tangential lamellae coexist with radial ones and the spherulite has a crosshatched texture.[1–6] Tangential lamellae, in which the chains lie nearly perpendicular to the radii of the spherulites, are thinner than radial lamellae and melt first. In the intermediate crystallization temperature range, 134–138°C, spherulites display mixed character,[2] and it is reported that most bulk crystallized samples fall into this category.[4] A range of spherulite types will be present if the crystallization temperature is not constant. Slightly different regime limits for the temperatures of crystallization are reported in later articles, and these differences are attributed to differences in the polymer specimens.[4,7]

Keith and Padden[2] found that mixed α spherulites became negatively birefringent when heated, indicating the removal of the tangential lamellae. The spherulite morphology attained at the annealing temperature remained as the sample cooled. Annealing causes the semicrystalline morphology to coarsen,[8] the crystallinity to rise,[9] and gives a narrower distribution of lamellar sizes.[8] The size of spherulite, however, is expected to remain unchanged.

The primary process in the interaction of radiation with polymers is the formation of excited

Correspondence to: R. E. Cameron.
Contract grant sponsor: British Nuclear Fuels Ltd.

Journal of Applied Polymer Science, Vol. 74, 2234–2242 (1999)
 CCC 0021-8995/99/092234-09

species, leading to the breakdown of chemical bonds and to the production of free radicals. The radicals thus produced, can react, resulting in crosslinking or chain scission, to change the chemical structure of the polymer molecule.[10,11]

In the presence of air, polypropylene subjected to gamma irradiation undergoes oxidative degradation causing scission and crosslinking.[11] In this polymer, chain scission as a result of gamma irradiation is generally believed to be similar to photo-oxidation, as evidenced by formation of carbonyl groups, which are typical products from chain scission.[12] The radiation-induced crosslinking, on the other hand, is a result of termination between polymer radicals formed. Postirradiation aging occurs as free radicals formed during irradiation react after the irradiation has ceased.[13] It is widely reported that radiation introduces major deterioration in mechanical properties of polypropylene as a consequence of the chain scission and crosslinking.[14–19]

A number of studies have indicated that changing the crystallinity or other morphological features can affect the response of polypropylene to radiation-induced degradation. The smectic mesomorphic phase of polypropylene, obtained by fast quenching from high-temperature melts, has been shown to withstand much higher doses of irradiation before mechanical property deterioration than the α monoclinic form.[15,16,18] Resistance to mechanical property deterioration under irradiation has also been linked with a high density of tie molecules between crystals and small spherulite size.[15]

The purpose of the research in this article is to investigate the effects of initial morphology on the response of polypropylene to γ irradiation. Identification of features of morphology that confer radiation stability will help enable better specification of polymers for applications where they will be subjected to irradiation.

MATERIALS

Isotactic polypropylene of average molecular weight, M_w, 250,000 was obtained from Sigma Aldrich Company Ltd. The powder was compression molded into plaques 1 mm thick and 160 mm square by first heating to 190°C and holding for 10 min, then increasing the molding pressure to 3 MPa. The temperature was maintained at 190°C for a further 10 min, although the pressure was allowed to fall. The mold and polymer were then plunged into a large bath filled with water maintained at about 10°C. Some samples were then annealed in a nitrogen atmosphere for 30 min at either 147 or 157°C to create samples with different lamellar morphologies.

Gamma irradiation was carried out by the Atomic Energy Authority using a ^{60}Co γ-ray source. Samples were sealed in glass tubes filled with air, and were irradiated up to doses of 50 kGy at a rate of 160 kGy/h at approximately 20°C. To minimize postirradiation effects, specimens were stored at −26°C (well below the glass transition temperature of the polymer[20]) after completion of the irradiation.

EXPERIMENTAL

Fourier Transform Infrared Spectroscopy

Fourier Transform Infrared Spectroscopy (FTIR) scans were performed using a Perkin-Elmer FTIR model 1720X in the transmission mode. Spectra obtained were the result of 100 scans. All data were normalized by setting the absorbance at 2428 cm^{-1} to 1.5.

Small-Angle X-ray Scattering

Small-angle X-ray scattering (SAXS) profiles were obtained from station 8.2 of the CLRC Daresbury Laboratory, UK, using a multiwire gas-filled proportional quadrant detector and a camera length of about 3 m. Data was divided by the detector response, as measured from uniform illumination of the detector by a ^{55}Fe source, normalized to a signal from an ionization chamber placed behind the sample, and a background profile subtracted. The scattering angle was calibrated using wet rat-tail collagen. The data was Lorentz corrected by multiplying the intensity by the square of the scattering angle. Peak positions were then obtained.

Wide-Angle X-ray Scattering

Wide-angle X-ray scattering (WAXS) profiles were obtained using a Phillips PW 1050/25 Automatic Powder Diffractometer, driven by the Phillips 1710 software system. The scattering angle, 2θ, was scanned from 4 to 50° at intervals of 0.02° at 40 kV and 40 mA. The scattering angle was calibrated using a silicon standard. Specimens of dimensions of 30 × 25 mm were cut from polypropylene sheets. Corrections were applied for errors

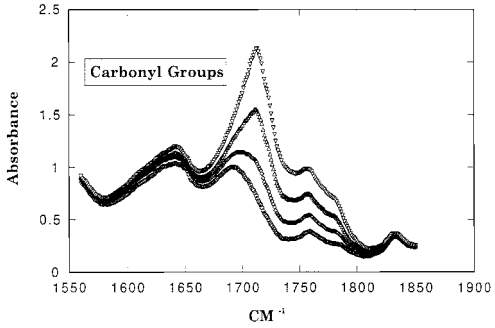

Figure 1 The FTIR spectra of nonannealed polypropylene irradiated to 0 (circles), 10 (diamnonds), 30 (up triangles), and 50 (down triangles) kGy scanned in the region of 1660–1800 cm^{-1} corresponding to carbonyl groups and similar organic species. It is clear that the concentration of these species increases with dose.

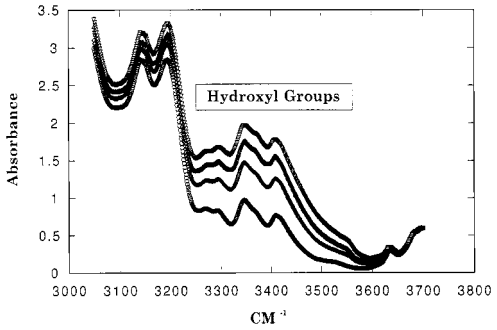

Figure 2 The FTIR spectra of nonannealed polypropylene irradiated to 0 (circles), 10 (diamnonds), 30 (up triangles), and 50 (down triangles) kGy scanned in the region of 3050–3600 cm^{-1} corresponding to hydroperoxide and hydroxyl groups and similar organic species. It is clear that the concentration of these species increases with dose.

in 2θ arising from the use of a flat specimen and from penetration of the primary beam.[21] The software was used to fit peaks to the crystal reflections and the broad amorphous halo, and the sample crystallinity was calculated from the ratio of the areas under the crystalline peaks to the total area. Peak positions and full-width at half maximum (FWHM) were also recorded.

Dynamic Mechanical Thermal Analysis

Dynamic mechanical thermal analysis (DMTA) was conducted on a Polymer Laboratories DMTA instrument. Samples of dimension 1 × 10 × 30 mm were tested in the bending mode at a heating rate of 3°C/min from −50 to 160°C, at frequency of 1 Hz.

Tensile Testing

Mechanical tests were performed using an ESH Testing Limited apparatus equipped with a 500N load cell. The tests were conducted at a constant crosshead speed of 10 mm/min at 22°C. The specimens were dumbbell-shaped tensile bars, milled such that the width was 3.5 mm and the gauge length 12 mm.

RESULTS AND DISCUSSION

Analysis of Chemical Groups

Figure 1 shows the FTIR spectra in the region of 1660–1800 cm^{-1} corresponding to carbonyl groups and similar organic species obtained from nonannealed polypropylene irradiated to 0, 10, 30, and 50 kGy. Figure 2 shows the spectra from these samples in the region of 3050–3600 cm^{-1}, corresponding to hydroperoxide and hydroxyl groups. All these groups are the products of polypropylene oxidation and, as would be expected from the literature, the concentration of these species increases with irradiation dose.[12,22,23]

Figure 3 shows the spectra in the region of 1660–1800 cm^{-1} from nonannealed samples and samples annealed at 147 and 157°C irradiated to doses of 0 and 50 kGy. There is exact superposition of the curves at 0 kGy, indicating that the annealing treatment itself did not introduce any oxidation. Further, there is minimal difference between the irradiated samples that received dif-

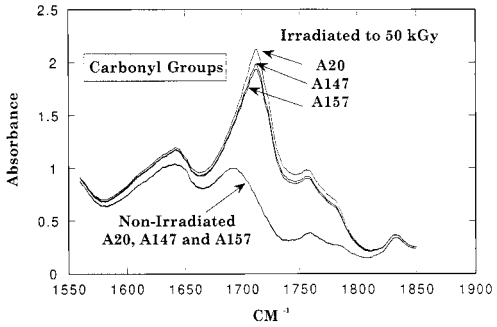

Figure 3 The FTIR spectra of nonannealed polypropylene and polypropylene annealed at 147 and 157°C for 30 min, irradiated to 0 and 50 kGy, and scanned in the region of 1660–1800 cm^{-1} corresponding to carbonyl groups and similar organic species. Annealing does not introduce detectable oxidation, and the extent of oxidation after irradiation is not affected by the annealing pre-treatments.

ferent preprocessing. This was also observed at the intermediate doses. This indicates that the chemical changes introduced by irradiation are largely a function of dose alone, and that any morphological changes introduced by preannealing have little or no effect.

In summary, the extent of oxidation of the polymer chains increases as the dose increases, but is largely unaffected by the starting morphology. This is important, as any differences in the responses of the annealed materials are, therefore, likely to be a consequence of morphological and not chemical differences between the samples.

Morphology

The surfaces of cryo-fractured nonirradiated samples, etched by sputtering in argon were examined by SEM. All the samples had very similar spherulitic morphology with spherulite radii in the approximate range 0.2–0.5 μm.

Figure 4 shows the Lorentz-corrected SAXS intensity profiles of the nonirradiated samples. Annealing causes the long period to increase (Table I) and the peak shape to narrow. Figure 5 shows the WAXS intensity profiles of the nonirradiated samples. The monoclinic α crystalline isomorph is dominant in all samples. The unit cell size was unchanged by the treatments used, but annealing causes the crystallinity to increase, and the FWHM of the (110) peak to fall (Table I). The values of the long spacing from the SAXS profile and those of the crystallinity from the WAXS profile may be combined to give an approximate indication of the average thickness of the crystal and amorphous layers, lc and la, respectively (Table I). Both lc and la rise.

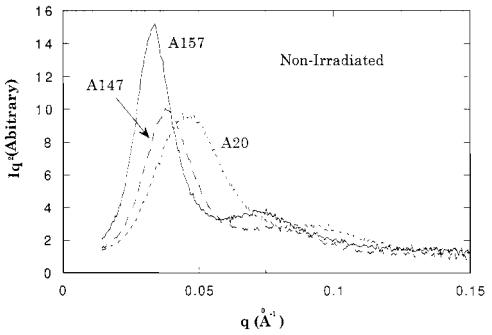

Figure 4 The Lorentz-corrected SAXS intensity profiles obtained from samples (a) that were compression molded but not annealed (A20), (b) annealed for 30 min at 147°C (A147), and (c) annealed for 10 min at 157°C (A157). Annealing narrows the peak and causes it to move to lower angles.

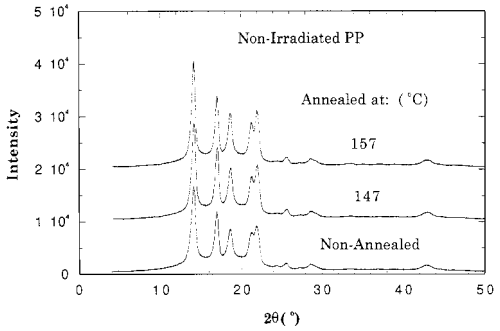

Figure 5 The WAXS intensity profiles of the nonirradiated samples (a) that were compression molded but not annealed, (b) annealed for 30 min at 147°C, and (c) annealed for 30 min at 157°C. The monoclinic α polymorph dominates in all samples, and annealing causes the crystallinity to rise.

These findings illustrate the coarsening of the lamellar structure, the narrowing of the distribution of lamellar sizes,[8] and the increase in the crystal size and perfection associated with annealing. The nonannealed samples are likely to contain a proportion of tangential lamellae in the spherulite because of the fast speed of cooling.[4] Annealing at 147 and 157°C is likely to result in a structure of predominately radial lamellae.[2]

Figure 6 shows the effect of irradiation on the Lorentz-corrected SAXS intensity profiles. The peak positions and, hence, the long spacings are largely unchanged by irradiation, and the peak intensity generally falls. Figure 7 shows the crystallinity obtained from the WAXS profiles from all samples. Irradiation causes a very slight increase in the crystallinity. Figure 8 illustrates the effect of irradiation on the values of the crystal and amorphous layer thickness assuming a two-phase model. The changes are not large, but there is a very small amount of crystallization and consequent thickening of the crystalline layer at the expense of the amorphous layer as a result of irradiation.

The crystallization is probably due to reorganization of polymer chains facilitated by chain scission. The increase in crystallinity is in contrast to the results of Yoda[24] on PEEK, which showed a reduction in the average crystal thickness of 15% after high irradiation doses, interpreted as being due to crosslinking near to lamellar surfaces. However, it is similar to the increase in crystallinity reported by Mani et al.[25] in isotactic polypropylene subjected to ultraviolet irradiation.

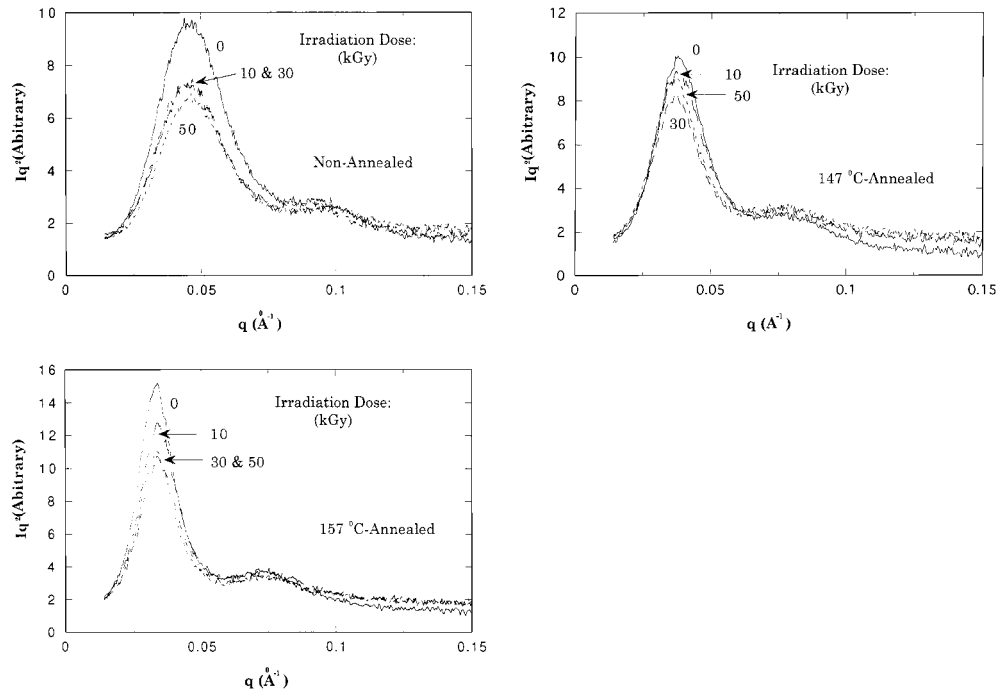

Figure 6 The Lorentz-corrected SAXS intensity profiles obtained from samples (a) that were compression molded but not annealed, (b) annealed for 30 min at 147°C, and (c) annealed for 10 min at 157°C, all irradiated to a dose of 0, 10, 30, and 50 kGy. Irradiation has a minimal effect on peak position, but does cause a drop in intensity.

The fall in intensity of the SAXS pattern on irradiation may be caused by several factors. The increase in crystallinity away from 50% (which gives maximum scatter) will be a contributory factor. Further, changes in the interface between crystalline and amorphous layers also have an effect on the overall scattering power and may contribute. The drop in scattering power could also be a consequence of a reduction in the electron density difference between the crystalline and amorphous layers. This could take the form of a reduction in the electron density of the crystalline phase (through the creation of defects within the crystal), or a densification of the amorphous phase (through improved packing after chain scission), or both.

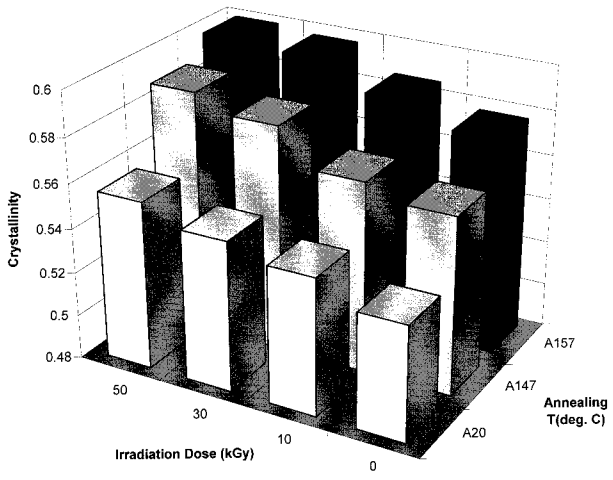

Figure 7 The crystallinity obtained from the WAXS profiles from all samples as function of annealing temperature and irradiation dose. Irradiation causes a very slight increase in the crystallinity for all starting morphologies. A20 indicates the nonannealed sample.

In summary, there appear to be small changes in morphology associated with irradiation, but these changes are tiny compared with the changes brought about by preannealing. The changes in response to irradiation appear to be similar for all three starting morphologies, despite the differences in lamellar architecture, and the probable differences in the proportions of radial and tangential lamellae and tie chain density.

Thermal Analysis

Figures 9(a) shows tan δ obtained from DMTA at 3°C/min at 1 Hz from each starting morphology

before irradiation. The peak seen between 0 and 20°C has been referred to in the literature as the β-transition, and represents the glass transition.[26] Its relaxation strength falls with annealing, suggesting that the amount of amorphous material falls, a result consistent with the rise in crystallinity measured by WAXS. The position of the β-transition is largely unchanged by annealing, indicating that the amorphous chains have similar mobility in each material.

The peak in tan δ between 50 and 150°C has been termed the α-relaxation, and has been interpreted as a consequence of relaxation mechanisms within the crystal phase.[25] The relaxation strength may be slightly larger for the annealed material, again indicating a higher crystallinity, although the effect is not great.

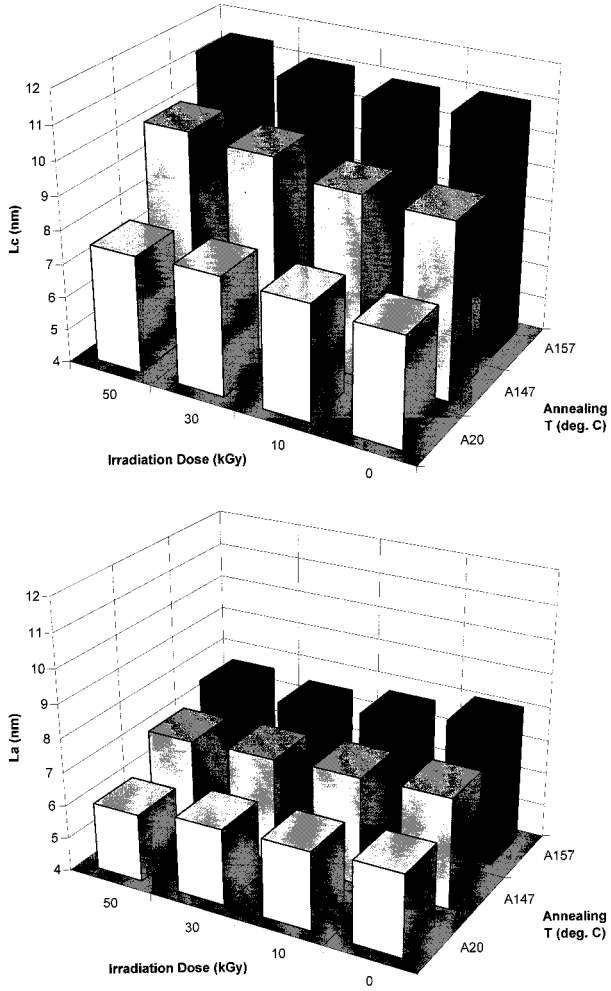

Figure 8 The values of (a) the average crystal lamellar thickness, lc, and (b) the average amorphous layer thickness, la, for all samples as function of annealing temperature and irradiation dose. Irradiation causes lc to rise slightly and la to fall slightly, but the overall change is very small. A20 indicates the nonannealed sample.

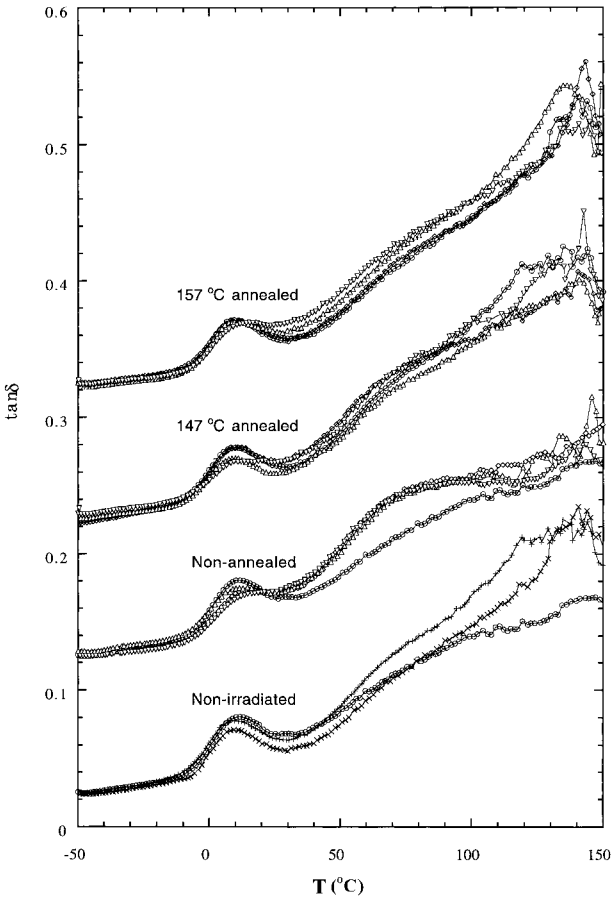

Figure 9 Values of tan δ obtained from DMTA as described in the text, in the temperature range of 50 to 120°C. (a) For nonirradiated samples (i) compression molded but not annealed (circles), (ii) annealed for 30 min at 147°C (+), and (iii) annealed for 10 min at 157°C (X). (b) For samples compression molded but not annealed, and irradiated to 0 (circles), 10 (up triangle), 30 (diamonds), and 50 (down triangles) kGy. (c) For samples annealed at 147°C for 30 min, and irradiated to 0 (circles), 10 (up triangle), 30 (diamonds), and 50 (down triangles) kGy. (d) For samples annealed at 157°C for 30 min, and irradiated to 0 (circles), 10 (up triangle), 30 (diamonds), and 50 (down triangles) kGy. Curves (b) to (d) have been offiset by multiples of 0.1 for clarity.

Figure 9(b)–(d) shows the value of tan δ obtained from samples irradiated to 0, 10, 30, and 50 kGy for all the samples. Irradiation causes the strength of the glass transition to fall slightly and its temperature to increase by a few °C; the strength of the α-relaxation also rises. These effects are particularly clear in the case of the nonannealed material [Fig. 9(b)].

The changes to the β-relaxation indicate that irradiation causes a drop in the amount of amorphous material free to relax, and constrains the remaining chains, increasing the relaxation temperature. The small rise in the glass transition temperature and the implied additional constraint of the amorphous chains is likely to be a result of both crosslinking and crystallization. Although the crystallization caused by annealing does not measurably change the transition temperature (Fig. 8), crystallization during irradiation occurs under at much lower temperatures (20°C), precluding large-scale chain rearrangement, and could well be expected to have a greater effect on chain constraint. Crosslinking is also known to occur, so both effects could be responsible for the rise in T_g. The starting morphology appears to have very little effect on the magnitude of the changes observed in T_g after irradiation (Fig. 10).

The reason for the increase in strength of the α-relaxation on irradiation is unclear. The increase in crystallinity indicated by WAXS (Fig. 7) will certainly contribute. However, this alone cannot account for the increase, as the strength is apparently larger than that seen in the more crystalline annealed samples. Chain scission may also play a role. Scission of tie chains in the amorphous phase could release constraints imposed on the crystals, facilitating relaxation.

The sizes of relaxation shown in Figure 9 more or less reflect the morphological changes. However, sample clamping and alignment may introduce some uncertainty in the data, particularly at high temperatures.

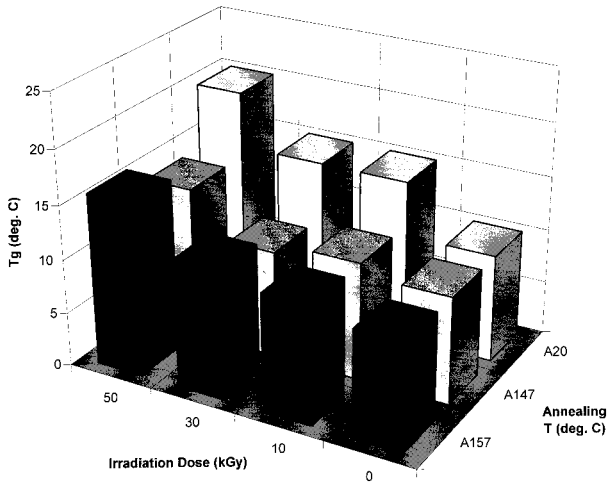

Figure 10 Approximate T_g values measured by DMTA of all samples as function of annealing temperature and irradiation dose. Irradiation causes a small increase in the glass transition temperature for all starting morphologies. A20 indicates the nonannealed material.

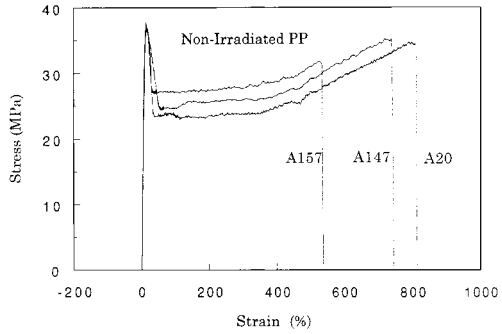

Figure 11 Tensile stress plotted against strain obtained at room temperature as described in the text for nonirradiated samples (a) compression molded but not annealed, (b) annealed for 30 min at 147°C, and (c) annealed for 10 min at 157°C. Annealing causes the strain to failure to fall.

In summary, irradiation appears to increase the strength of the α-transition while weakening the glass transition and moving it to higher values, effects that can be related to the changing crystallinity and chemistry. The annealing treatments used change the relative strengths of the peaks as crystallization occurs, but have little or no effect on their position. The changes in response brought about by irradiation are broadly similar for each starting morphology.

Mechanical Properties at Room Temperature

Figure 11 shows the stress–strain curves obtained for the nonirradiated samples. The expected form of curve is obtained. The Young's modulus, yield stress, and strain at break are shown in Table I. As expected, the higher crystallinity of the annealed samples results in samples with a higher Young's modulus and a lower strain at break. The yield stress appears to be unaffected by the annealing process used in this study, and remains almost constant.

The stress–strain curves obtained from unannealed material irradiated to 0, 10, 30, and 50 kGy are shown in Figure 12. Curves of similar shape were obtained for the annealed samples and Figures 13 and 14 show the values of Young's modulus and strain at break obtained.

The Young's modulus of the samples rises with increasing dose. This is likely to be a consequence of the increased crystallinity and crosslinking. The stiffness will increase slightly as a result of

Table I Morphology and Mechanical Parameters of Nonirradiated Material

Annealing T (°C)	Long Spacing (nm)	Crystallinity (%)	lc (nm)	la (nm)	E (GPa)	σ_y (MPa)	ε_b (%)
Nonannealed	13.8	53.2	7.3	6.5	0.48 ± 0.05	37.3 ± 0.6	680–808
147	16.6	56.0	9.3	7.3	0.53 ± 0.05	37.0 ± 0.3	578–746
157	19.1	57.7	11.0	8.1	0.59 ± 0.05	37.1 ± 0.5	538–542

the slightly greater crystallinity of the irradiated samples. Further, the increased constraint of the amorphous phase arising from crystallization and crosslinking, illustrated by the rise in T_g seen by DMTA, also contributes. These effects apparently dominate over any reduction in Young's modulus as a consequence of chain scission.

The irradiated samples do not deform plastically under the deformation conditions imposed, and fail at much lower strains. This transition from ductile to brittle deformation is likely to be the result of both chain scission—which gives a material that cannot retain connectivity on drawing—and crosslinking—which retards plastic deformation. During the tensile tests of samples irradiated to doses in excess of 10 kGy, surface cracks preceded brittle fracture. These surface cracks were perpendicular to the loading direction and traversed the tensile bar, and the resultant stress concentration led to brittle failure. Oxidation will be more severe at the surface of a sample, owing to diffusion effects,[12] and this would favor the formation of these cracks. It is possible that the leveling off of the curve of the apparent Young's modulus with dose at high doses is a consequence of changes in the geometry associated with these cracks.

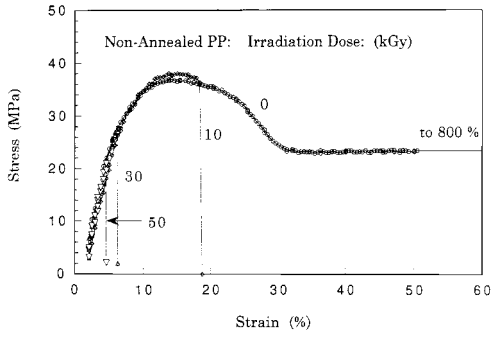

Figure 12 Tensile stress plotted against strain obtained at room temperature as described in the text for nonirradiated samples compression molded but not annealed, and irradiated to 0, 10, 30, and 50 kGy. The irradiated samples all fail in a brittle manner.

In summary, irradiation causes the material to fail in a brittle manner, and results in an increase in the Young's modulus and a fall in the strain at break, a consequence of the increased crystallinity, crosslink density, and lowered molecular weight. The changes in Young's modulus on irradiation are greater for the preannealed samples, but little difference in strain at break is observed between different starting morphologies, all samples failing at low strains.

CONCLUSIONS

This article explores the effects of irradiation on isotactic polypropylene, together with the effects of starting morphology on the phenomena observed. FTIR results show that chain scission occurs and that the degree of chemical change is unaffected by the starting morphologies introduced. These changes cause the crystallinity to increase slightly and the glass transition temperature to rise by a few degrees in all samples, but

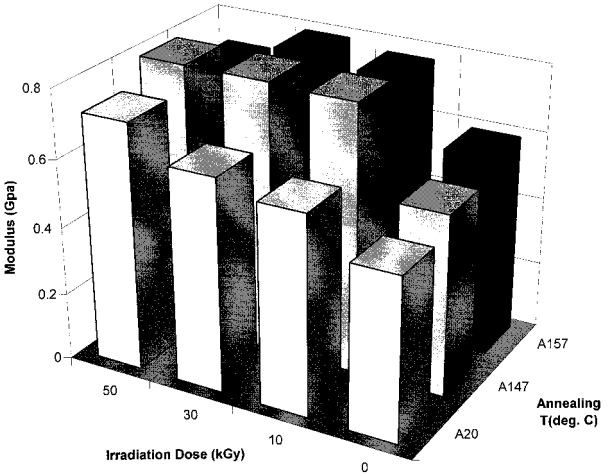

Figure 13 Modulus as function of annealing temperature and irradiation dose. Values are the average of three readings. Irradiation causes the modulus to rise in all samples. A20 indicates the nonannealed sample.

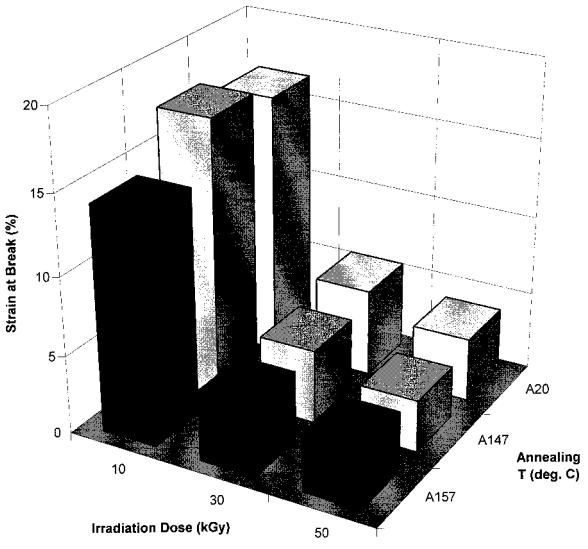

Figure 14 Strain to failure s function of annealing temperature and irradiation dose. Values are the average of three readings. Irradiation causes the strain to failure to fall in all samples. A20 indicates the nonannealed sample.

the overall morphology is affected only slightly. There are only subtle changes in the dimensions of the lamellar architecture. Radiation does, however, introduce major deterioration in mechanical properties. The changes to morphology on irradiation all occur similarly in the annealed materials and to similar amounts. The ultimate properties after irradiation are determined by the properties seen in the original material.

The results in this article are concerned with the small changes in morphology on irradiation and the deformation of the samples at room temperature, when all the irradiated samples behave in a brittle manner. Clearly, irradiation raises the ductile–brittle transition of these materials to a value above room temperature, but the details of the effect are not shown by these experiments. In separate articles[27,28] we report simultaneous SAXS/tensile deformation experiments using synchrotron radiation, exploring the micromechanisms of degradation before and after the ductile–brittle transition, and the effects of the initial morphology on the transition temperature after irradiation.

The authors are grateful to British Nuclear Fuels Ltd. who funded this research. The SAXS data was obtained on station 8.2 of the CLRC Daresbury Laboratory with the help and advice of Dr. B. U. Komanscheck. Software from the CCP13 suite was employed in the data analysis.

REFERENCES

1. Varga, J. Polypropylene: Structure, Blends and Composites; Karger Kocsis, J., Ed.; Chapman and Hall: London, 1995.
2. Padden, F. J., Jr.; Keith, H. D. J Appl Phys 1959, 30, 1479.
3. Padden, F. J., Jr.; Keith, H. D. J Appl Phys 1973, 44, 1217.
4. Norton, D. R.; Keller, A. Polymer 1985, 26, 705.
5. Lotz, B.; Wittman, J. C. J Polym Sci Polym Phys Ed 1986, 24, 1541.
6. Olley, R. H.; Bassett, D. C. Polymer 1989, 30, 399.
7. Idrissi, M. O. B.; Chabert, B.; Guilliet, J. Makromol Chem 1985, 186, 881.
8. O'Kane, W. J.; Young, R. J.; Ryan, A. J. J Macromol Sci Phys 1995, B34, 427.
9. Frontini, P. M.; Fave, A. J Mater Sci 1985, 30, 2446.
10. Nishimoto, S.; Kagiya, T. Handbook of Polymer Degradation, Chapter 1: Radiation Degradation of Polypropylene; Hamid, S. H.; Amin, M. B.; Maadhah, A. G., Eds.; Marcel Dekker: New York, 1992.
11. Carlsson, D. J.; Chmela, S. Mechanisms of Polymer Degradation and Stabilisation, Chapter 4: Polymers and High-Energy Irradiation: Degradation and Stabililisation; Scott, G., Ed.; Elsevier: London, 1990.
12. Gillen, K. T.; Clough, R. L. Irradiation Effects on Polymers; Clegg, D. W.; Collyer, A. A., Eds.; Elsevier: New York, 1991.
13. Carlsson, D. J.; Dobbin, C. J. B.; Jensen, J. P. T.; Wiles, D. M. ACS Symp Series 1985, 280, 25.
14. Kagiya, T.; Nishimoto, S.; Watanabe, Y.; Kato, M. Polym Degrad Stabil 1985, 12, 261.
15. Nishimoto, S.; Kitamura, K.; Watanabe, Y.; Kagiya, T. Radiat Phys Chem 1991, 37, 71.
16. Rolando, R. J. J Plastic Film Sheeting 1993, 9, 326.
17. Martakis, N.; Niaonakis, M.; Pissimissis, D. J Appl Polym Sci 1994, 51, 313.
18. Nishimoto, S.; Kagiya, K.; Watanabe, Y.; Kato, M. Polym Degrad Stabil 1986, 14, 199.
19. Kholyou, F.; Katbab, A. A. Radiat Phys Chem 1993, 42, 219.
20. McCrum, N. G.; Read, B. E.; Williams, G. Anelastic and Dielectric Effects in Polymeric Solids; Dover: New York, 1991.
21. Balta-Calleja, F. J.; Vonk, C. G. X-ray Scattering of Synthetic Polymers; Elsevier: New York, 1989.
22. Charlesby, A. Atomic Radiation of Polymers; Pergamon: London, 1960.
23. Faucitano, A.; Buttafava, A.; Camino, G.; Greci, L. Trends Polym Sci 1996, 4, 92.
24. Yoda, O. Polym Commun 1985, 26, 16.
25. Mani, R.; Singh, R. P.; Sivaram, S.; Lacoste, J. Polym J 1994, 26, 1132.
26. Ishigaki, I.; Yoshii, F. Radiat Phys Chem 1992, 39, 527.
27. Zhang, X. C.; Butler, M. F.; Cameron, R. E. Polymer, in press.
28. Zhang, X. C.; Butler, M. F.; Cameron, R. E. Polymer International, in press.